DESIGN OF A POWER SUPPLY CAPABLE OF DRIVING A DIVERSE SET OF DBD EXCILAMPS

A. Wiesner, R. Diez, D. Florez, Hubert Piquet

DESIGN OF A POWER SUPPLY CAPABLE OF DRIVING A DIVERSE SET OF DBD EXCILAMPS

A. Wiesner[1,2], R. Diez[1], D. Florez[1,3], H. Piquet[2]

1. Pontificia Universidad Javeriana, Carrera 7 No. 40-62, 110231 Bogotá, Colombia
2. LAPLACE, Université de Toulouse, CNRS, INPT, UPS, 2 rue Charles Camichel, 31071 Toulouse, France
3. Universidad Sergio Arboleda, Calle 74 No. 14-14, 110221 Bogotá, Colombia

E-mail: wiesner@laplace.univ-tlse.fr

Abstract – In this work the procedure to design a power supply capable of supplying nineteen different exciplex Dielectric Barrier Discharge (DBD) UV lamps, is shown. This power supply is studied with the aim to study the impact of the DBD lamp geometrical characteristics over system's performances (UV emission, efficiency). The pulsed power supply can control and adjust three electric parameters: frequency, amplitude and duration of the current pulses. For this reason, a wide operating range is needed and the choice of the elements for the power supply is a challenge. Modeling of the lamps is used to define the most interesting operating points to be explored and also for the selection of the devices ratings and the parameters of the supply (semiconductors, control, transformer).

Keywords – DBD, exciplex, power converter, current mode.

1. INTRODUCTION

Dielectric Barrier Discharge (DBD) UV lamps are environmentally friendly (mercury free) UV sources with various applications: disinfection, microelectronics, surface treatments, health. The practical usefulness and applicability of currently available DBD excilamps has been demonstrated [1]; today, studies oriented toward their performance improvement are in development. This can be achieved by means of the reactor design optimization (geometry, filling mixture, pressure and materials) [2], [3] and also by choosing the most performing electrical operating conditions [4], [5].

The impact of the electrical operating point (OP) over the DBD excilamps performance has been already reported by different teams [1], [7] and [6]. However, because a DBD excilamp design cannot be easily adjusted [8] and constructed, most of these studies are developed for a fixed lamp design and the impact of the DBD lamp geometry over the lamp performance has not been widely reported.

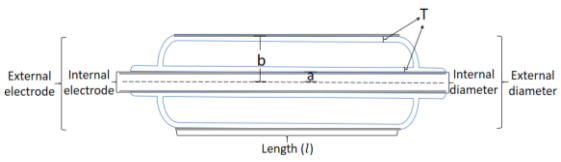

Fig. 1. DBD lamp geometry

With the aim to provide deeper insight and experimental evidence about the impact of the geometry of the DBD reactor, a set of nineteen diverse DBD exciplex UV lamps of coaxial type, has been built, as shows the Fig. 1: *T* is the dielectric thicknesses, *a* is the internal radius, *b* is the external radius and *l* is the length of the lamp. Each one of the 19 bulbs present a different parameter set *{T, a, b, l}*; these lamps were designed and manufactured, differing among them in their dielectric thicknesses and clearances (gas gap), and filled with the same gas mixture.

The proposed study consists on supplying the different excilamps at different controlled electrical operating points, comparing the lamp performances in terms of the obtained UV power and of the system's electrical power to UV power efficiency; for each experiment, the parameters of the electrical model of the bulb are identified.

From previous works a significant impact of the lamp operating point over the lamp performance has been evidenced. Particularly, the methodology proposed in [5] makes use of a square-shape current waveform for the parametric study of DBDs. By means of the i_{DBD} current waveform, the lamp power can be controlled with three degrees of freedom: duty cycle (*D*), current intensity (*J*) and frequency (*f*) of the current pulses, as show in Fig. 3.

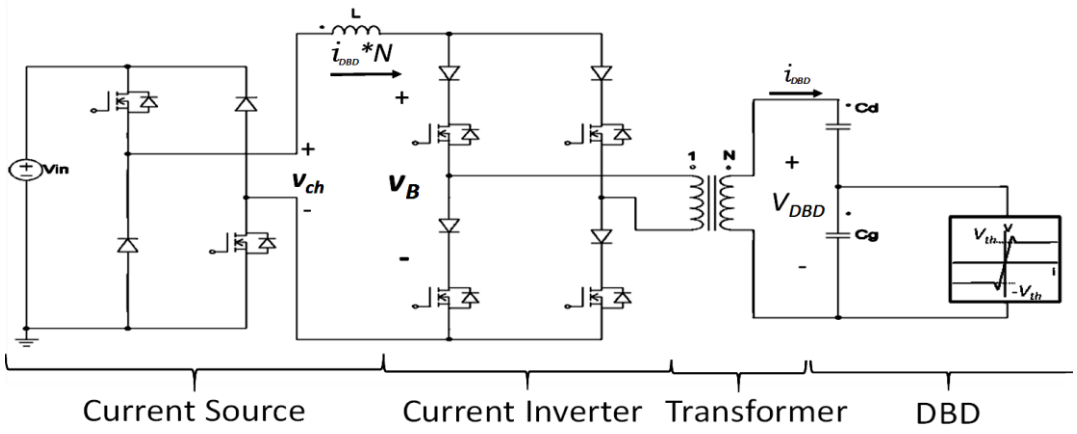

Fig. 2. DBD power supply.

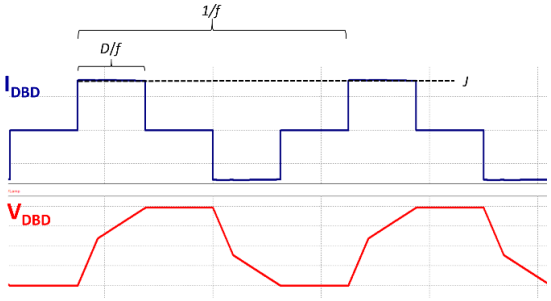

Fig. 3. DBD current and voltage waveforms using a square-shape current source.

The topology of the power supply consists in a constant current source connected in cascade to a full-bridge inverter [5], as shown on Fig. 2. A step-up transformer is used to connect the bulb to the current inverter. The dimensioning and implementation of this converter for the current study is a challenge due to the wide range of operating conditions implied by the set of 19 lamps. According to the dimensions of the bulbs the power range of this supply from has been chosen from 0 to 500W.

This design process is presented as follows: first, the electrical model of each lamp is theoretically obtained as a basis for the converter design. Then, using these models and taking into account the different characteristics of the 19 bulbs, the operating range of interest, concerning the properties of the current pulses, is determined. Finally, the converter design is presented, pointing out the challenges of supplying such a different set of loads and at this level of power (up to 500W).

2. DBD LAMPS UNDER STUDY

The nineteen coaxial DBD lamps, used for this work, present the configuration shown in Fig. 1 and have different geometrical parameters that are categorized as:

- External diameter: with two different values, *25mm* and *45mm*.
- Internal diameter: six different values varying from *5mm* to *30mm* in steps of *5mm*.
- Thickness of the dielectric barriers: three different values, *1*, *1.5* and *2mm*. The inner and outer barrier thickness is the same for each lamp.

All the lamps have a length (l) of *600mm*. The gas mixture used to fill the lamp bulbs is *XeCl*, producing a radiation wavelength at *308nm*.

In order to design a power supply capable of driving all the lamps under study, initially, the electrical magnitudes are calculated using the simplified electrical model of the DBD developed in [9], as shown in Fig. 4.

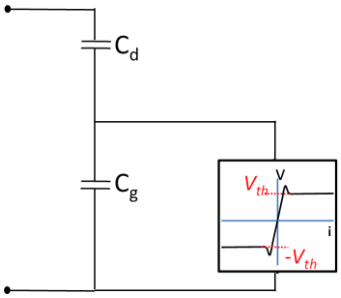

Fig. 4. DBD electrical model.

C_d is the dielectric series equivalent capacitance, C_g the gas equivalent capacitance and V_{th} the gas breakdown voltage. The lamp model parameters are estimated using the cylindrical capacitor equation (1) and (2), for the values of C_g and C_d and using the Paschen's law (3) for the breakdown voltage V_{th}.

$$C_g = \frac{2\pi \cdot \varepsilon_g . l}{In\left(\frac{b}{a}\right)} \approx y \frac{l}{In\left(\frac{b}{a}\right)} \qquad (1)$$

$$C_d = 2\pi \cdot \varepsilon_d \cdot l \cdot \frac{1}{ln\left(\frac{T^2 + a \cdot T + b \cdot T + a \cdot b}{a \cdot b}\right)}$$

$$C_d \approx z \cdot l \cdot \frac{1}{ln\left(\frac{T^2 + a \cdot T + b \cdot T + a \cdot b}{a \cdot b}\right)} \quad (2)$$

$$V_{th} = \frac{C \cdot p_{gas} \cdot d}{In\left(\frac{A \cdot p_{gas} \cdot d}{In\left(1 + \frac{1}{\gamma}\right)}\right)} \approx X \frac{d}{In(d)} \quad (3)$$

a, b, l and *T* are the geometrical parameters of the lamp; *A* is a constant which depends on the electron kinetic temperature, *C* is related to *A* and to the effective ionization potential V^* ($C=A\ V^*$), p_{gas} is the pressure, *d* is the distance between dielectrics, γ is the electron emission coefficient [10].

In these three equations, the y, X and z terms are constants, which values are derived from measurements achieved on a bulb with the same material for walls, gas mixture and pressure [8].

With the geometry known for each lamp, the values for the components of electrical model are calculated, obtaining the range in Table 1.

Table 1: Electrical values

	Range
Dielectric capacitance (C_d)	*34pF - 200nF*
Gas capacitance (C_g)	*96pF - 84nF*
Threshold voltage (V_{th})	*375V - 2400V*

3. OPERATING POINTS RANGE

In order to design the power supply, a maximum power value of *500W* is chosen. Once the electrical model for each lamp is obtained, it is possible to find out the values of the *J* amplitude of the lamp current (i_{DBD}) and the peak voltage for those lamps, thanks to equations (3) and (4), deduced from work detailed in [5].

$$J = \frac{P}{D \cdot V_{th}} + f\frac{4 \cdot C_g \cdot V_{th}}{D} \quad (4)$$

$$\hat{V}_{DBD} = V_{th} + \frac{J \cdot D}{4 \cdot f \cdot C_d} \quad (5)$$

P is the desired average electric power on the DBD; *D*, *J*, *f* are the three degrees of freedom of the i_{DBD} current shape, controlled thanks to the current inverter (*f*, *D*) and the current source (*J*N*, *N* being the turn ratio of the transformer). C_d, C_g, V_{th} are the DBD electrical model parameters.

Fig. 5 presents the current pulse amplitude *J*, obtained from eq(4), versus the *f* frequency for two different duty cycles (*D=5%* and *D=100%*) and for the maximum requested power (*P=500W*). As expected, the lower the duty cycle, the higher the *J* current amplitude. One can observe that the required power is obtained, for *D=100%*, with a relatively low *J* value (to remember, that this value will define the operating conditions of the current inverter and of the current source; these converters will have to control a *J*N* current, *N* being the turn ratio of the transformer). In order to avoid oversizing of the current converters, the maximum *J=1.6A* value has been selected. As a matter of fact, almost all the points associated with the *D=5%* duty ratio will be unreachable (shadowed area). For the shadowed operating points, the specific power (power per unit of bulb's length), which is unreachable using the full length of the bulb, will be attained thanks to an outer metallic electrode of reduced length.

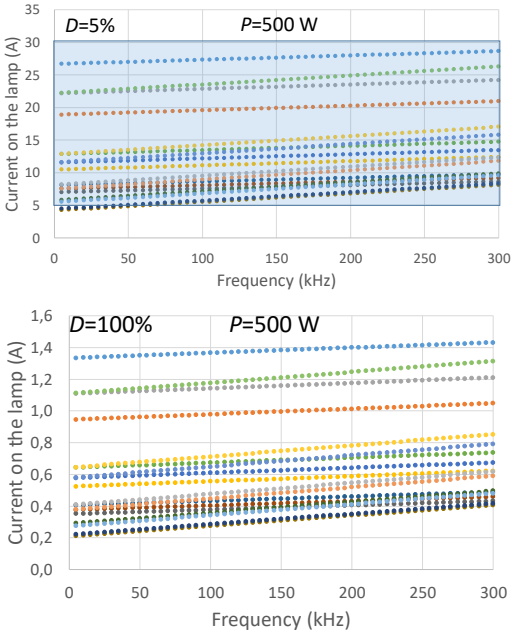

Fig. 5. Current in the 19 lamps as a function of the frequency. Cases for duty cycle of 5% (top) and 100% (bottom).

Combining eq (4) in eq(5), we obtain the following equation (6), where it appears that the lamp peak voltage ($\hat{V}_{DBD}$) does not explicitly depends on the duty cycle *D*.

$$\hat{V}_{DBD} = V_{th}\left(1 + \frac{C_g}{C_d}\right) + \frac{P}{f \cdot 4 \cdot C_d \cdot V_{th}} \quad (6)$$

For the same *P=500W* power level, Fig. 6 presents the lamp peak voltage ($\hat{V}_{DBD}$) versus frequency, for the 19 lamps.

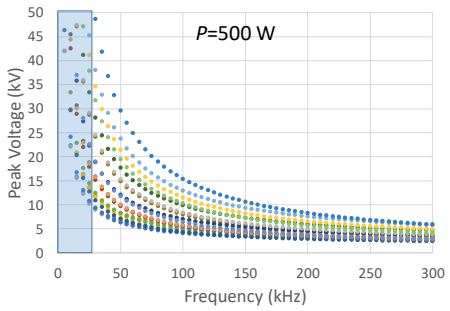

Fig. 6. Lamp peak voltage as a function of the frequency.

This figure shows that the requested lamp voltage in low frequencies is very high. To avoid oversizing of the step-up transformer, the minimum operating frequency has been limited to *30kHz*. The maximum operating frequency has been set to *200kHz* considering implementation aspects, as the speed of semiconductor devices and the limitation of magnetic materials.

To conclude this section, we summarize below the operating range of the parameters of the i_{DBD} pulses:

- $0 < J < 1.6A$
- $5\% < D < 100\%$
- $30kHz < f < 200kHz$

4. CONVERTER DESIGN

After finding the operating range for the 3 degrees of freedom to make the DBD characterizations, the system design is now achieved.

4.1 Inverter switch selection

The selection of the inverter switches is performed under the assumption that the power can be delivered to the lamp, independently of the turn ratio of the transformer that will be chosen later. For that purpose, the product of voltage and current in each lamp is obtained for the most demanding case, multiplying Fig. 5 (*D=100%*) and Fig. 6, resulting in the decaying curve shown in Fig. 7 for a given lamp.

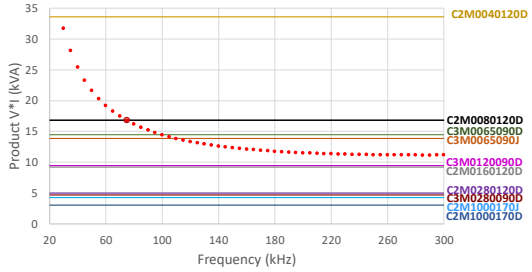

Fig. 7. Selection of the switches via the V I product.

The obtained curve is compared to the product of the blocking voltage and the current rating of the candidate switches for the converter (flat lines in Fig. 7). The operating points that are above the intersection between the lamp and switch curves are the ones that cannot be attained by the switch, regardless of the transformer ratio to be chosen.

The switch is chosen using a compromise between its price and the number of reachable OP. Fig. 6 is useful to determine the value of the minimum operating frequency for the selected switch.

4.2. Transformer

Once the switches have been chosen, the interesting OPs from Fig. 7 are tested for different transformer's turn ratios (N). The points to be discarded are the ones where the peak voltage or the current in the lamp (seen in the primary side of the transformer) exceeds the ratings of the switch. The points with power losses in the switches greater than *30W* are also removed, due to thermal limitation for the available cooling system (classical dissipators).

Fig. 8 shows the result of this analysis and the transformation ratio is selected maximizing the number of reachable points, but also assuring a wide frequency range. In this case a turn ratio of 10 is selected.

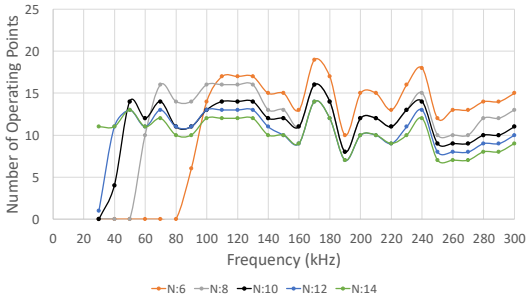

Fig. 8. Operating points attained vs. the frequency for different turns ratio of the transformer.

4.3. Current source

To avoid the influence of the i_{DBD} current ripple on the DBD performance, the frequency of the current source which supplies the current inverter should be much higher than the maximum frequency of the latter: the $f_{max}=200kHz$ selected value makes it impossible to satisfy this condition. For this reason, parallelized current choppers, with an interleaved configuration allow the reduction on the magnetic cores and increase the apparent frequency of the delivered current.

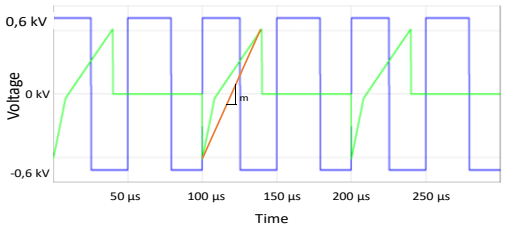

Fig. 9. output voltage of the chopper v_{ch} and input voltage of the current inverter v_B - case where f_{ch} is similar than f_B.

Therefore, the maximum frequency of the current sources is defined by the speed of semiconductor devices, switching losses and the limitation of magnetic materials. Thus the maximum frequency on the inverter and the maximum frequency on each current source are similar as shown in Fig. 10, This figure plots the output voltage of the chopper v_{ch} and the input voltage of the current inverter v_B.

Finally, the L inductor which controls the current ripple at the input of the current inverter is defined. In that scope, we use eq. (10). The current ripple on the L inductor is defined by:

$$\Delta i_L = \frac{1}{L}\int_{t}^{t+D_{ch}T_{ch}} V_{in}\,dt - \frac{1}{L}\int_{t}^{t+D_{ch}T_{ch}} v_B\,dt \qquad (7)$$

$$\Delta i_L = \frac{D_{ch}}{Lf_{ch}}\left(V_{in} - V_0 - \frac{mD_{ch}}{2f_{ch}}\right) \qquad (8)$$

Assuming the approximation of the shape of the v_B voltage, highlighted with the red slope (m) in Fig. 10, the current ripple is defined by:

$$m \approx \frac{2 \cdot V_p.f}{N \cdot D} \qquad (9)$$

$$\Delta i_L = \frac{D_{ch}}{L \cdot f_{ch}}\left(V_{in} - v_B - V_p \cdot \frac{f \cdot D_{ch}}{N \cdot f_{ch} \cdot D}\right) \qquad (10)$$

v_B is a variable voltage that varies between $-V_p$ and V_p as shown in Fig. 9, N is the turns ratio on the transformer, f and D are the frequency and duty cycle on the current inverter and f_{ch} and D_{ch} are the frequency and duty cycle on the current source. Note that this converter differs from conventional DC-DC converters, because v_B changes and it is dependent on the inverter frequency. This fact implies a high inductance value to maintain a low current ripple.

4.4. Working range

Once defined the different devices of the system, it is important to finally find out the actual possible OP for each lamp. In this scope, a cloud of accessible operating points is plotted: for each lamp, varying f in steps of *5kHz*, D in steps of *5%* and J in steps of *0.2A*.

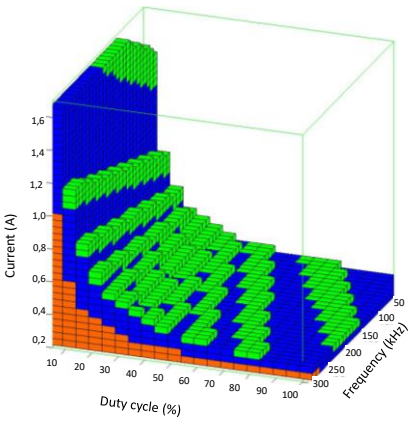

Fig. 10. Possible operating points and the ones that inject between 400 and 500 W of power, for one of the lamps.

In Fig. 10, we observe for one specific lamp that the three degrees of freedom form a cube with all possible OP: within this cube, the green cells are the most interesting OP for the experiment as their power lies between 400W and 500W. The blue cells are the ones that inject less than 400 W to the lamp.
The others are eliminated for various reasons: the orange ones are the OP which are not relevant, because these do not ignite the lamp. The white ones (blank spaces over the green or blue OP) are eliminated because one of the following conditions is fulfilled:

- the peak voltage across the switches is higher than their maximum allowed value;
- the peak voltage across the lamp exceeds the dielectric strength of the transformer insulation (not detailed in this paper);
- the power is higher than *500W*.

One should remember here that the peak voltages as well as the maximum power depend on the geometrical parameters (T, a, b, l) of the bulbs; for that reason, the cloud's shape and size change for each lamp.

5. SIMULATION AND EXPERIMENTAL TEST

To validate the theoretical analysis and evaluate the performance, the whole system is simulated in PSIM as shown in Fig. 11, and tested as shown in Fig. 12.

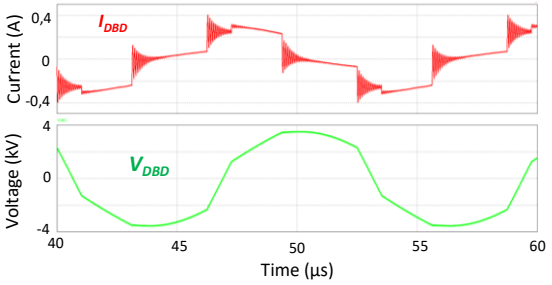

Fig. 11. Simulated waveforms for a specific case.

The curves displayed in Fig. 11, and Fig. 12 are for the OP with *f=80kHz*, *D=50%* and *J*=3*A*.

Fig. 12 shows the DBD current (i_{DBD}), the DBD voltage (V_{DBD}), and the total current (*J*N*) delivered by the two parallelized current choppers.

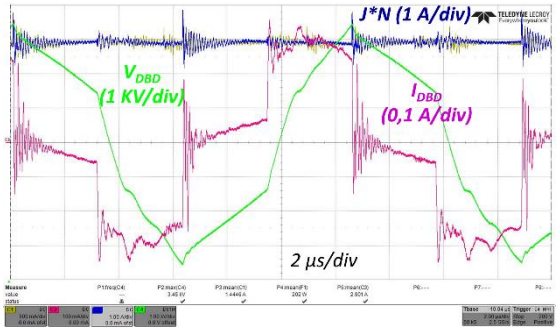

Fig. 12. *J*N* current, current (I_{c1}) and the voltage and current on the DBD to specific OP.

The simulation and the experimental test are in good agreement with the theoretical analysis, as shows Table 2.

Table 2: Results comparison

	Theoretical	**Simulation**	**Test**
$\hat{V}_{DBD}$	3.5 kV	3.5 kV	3.45 kV
P	166 W	171 W	202 W

6. CONCLUSIONS

The procedure to design a power converter capable of supplying 19 different lamps has been explained and proved. This method optimizes the number of OP for the set of DBDs.

The modeling of the lamps is necessary to perform the dimensioning of the power supply. The inverter switches are selected on the basis of a good balance between cost and the number of interesting operating points that are attainable.

The transformation ratio is also selected maximizing the interesting operating points that are attainable and the most desired frequency range.

According to the frequency range of the current pulses (f_{max}=*200kHz*), the realization of the DC current source, which needs to present an even higher frequency is a real challenge. In our opinion, with the current limitations of the semiconductors, the most relevant solution is the implementation of current source converters with interleaved switching: this enables a good reduction in the output current ripple and multiplies the apparent switching frequency.

ACKNOWLEDGEMENTS

The authors acknowledge specially to ECOS-Nord / COLCENCIAS / ICETEX French-Colombian cooperation program, ECOS Nord Program under Project C16P01, by Colciencias under contracts 663-2015 and 294-2016 and by Universidad Sergio Arboleda under Project IN.BG.086.16.013 and COLCENCIAS / COLFUTURO because part of this work is supported by them.

REFERENCES

[1] M. I. Lomaev, E. A. Sosnin, and V. F. Tarasenko, “Excilamps and their applications,” *Prog. Quantum Electron.*, vol. 36, no. 1, pp. 51–97, Jan. 2012.

[2] M. V. Erofeev, D. V. Schitz, V. S. Skakun, E. A. Sosnin, and V. F. Tarasenko, “Compact dielectric barrier discharge excilamps,” *Phys. Scr.*, vol. 82, no. 4, p. 045403, 2010.

[3] C. Blanco Viejo *et al.*, “Comparison Between Different Discharge Lamp Models Based on Lamp Dynamic Conductance,” *IEEE Trans. Ind. Appl.*, vol. 47, no. 4, pp. 1983–1991, Jul. 2011.

[4] M. Meißer, “Resonant Behaviour of Pulse Generators for the Efficient Drive of Optical Radiation Sources Based on Dielectric Barrier Discharges,” KIT Scientific Publishing, Karlsruhe, 2013.

[5] D. Florez, R. Diez, H. Piquet, and A. K. Hay Harb, “Square-Shape Current-Mode Supply for Parametric Control of the DBD Excilamp Power,” *IEEE Trans. Ind. Electron.*, vol. 62, no. 3, pp. 1451–1460, Mar. 2015.

[6] D. Florez, R. Diez, and H. Piquet, “Optimizing the Operation of DBD Excilamps,” *IEEE Trans. Plasma Sci.*, vol. 44, no. 7, pp. 1160–1168, Jul. 2016.

[7] M. I. Lomaev, V. S. Skakun, E. A. Sosnin, V. F. Tarasenko, D. V. Shitts, and M. V. Erofeev, “Excilamps efficient sources of spontaneous UV and VUV radiation,” *Phys.-Uspekhi*, vol. 46, no. 2, pp. 193–209, Feb. 2003.

[8] R. Díez, J.-P. Salanne, H. Piquet, S. Bhosle, and G. Zissis, “Predictive model of a DBD lamp for power supply design and method for the automatic identification of its parameters,” *Eur. Phys. J. - Appl. Phys.*, vol. 37, no. 03, pp. 307–313, 2007.

[9] R. Diez, H. Piquet, S. Bhosle and J. M. Blaquiere, "Current mode converter for dielectric barrier discharge lamp," *2008 IEEE Power Electronics Specialists Conference*, Rhodes, 2008, pp. 2485-2491.

[10] J Reece Roth, “Dark Electrical Discharges in Gases" in *Industrial Plasma Engineering British Library Cataloguing*, vol.1, pp. 251–296. 1995.